Increasing local density and purity of molecules/bacteria on a sensing surface from diluted blood using 3D hybrid electrokinetics

I-Fang Cheng,[1,a)] Tzu-Ying Chen,[1] and Wen-Cheng Chao[2,3]
[1]*National Nano Device Laboratories, National Applied Research Laboratories, Tainan, Taiwan*
[2]*Department of Medical Research, Taichung Veterans General Hospital, Taichung, Taiwan*
[3]*Institute of Clinical Medicine, National Cheng Kung University Medical College, Tainan, Taiwan*

(Received 5 April 2016; accepted 25 May 2016; published online 8 June 2016)

We present a long-range and selective nanocolloid/molecular/bacteria concentrator based on 3D hybrid AC electrokinetics (ACEK) that includes AC dielectrophoresis (DEP) and biased AC electroosmosis (ACEO). Through a convergency comb-shaped electrode design, this long-range ACEO allows the effective transport of a high number of targets into the centre of the detection zone. In the proposed 3D hybrid electrokinetics model, 3D ACEO provides long-range transportation, and the 3D DEP provides an effective separation mechanism. Thus, detection targets ranging from nanoscale to micrometers could be selectively concentrated long-range from diluted blood. The proposed design was used for selectively concentrating nanocolloids and bacteria in the diluted blood sample, respectively. Compared to a 3D short-range dipolar electrode configuration, the detection limit of long-range 3D convergency tripolar electrode configuration is one order of magnitude higher. The result also shows that the 3D hybrid ACEK demonstrated a higher purity of any plane above the electrode, which compared positively to the same design of a 2D hybrid ACEK. The concentration factor of the proposed 3D hybrid electrokinetics device increased by several orders of local density and raised the local purity at least 6 orders (from 0.05% to greater than 99.9%). The chip is capable of making a DNA/protein/bacterial aggregate characterized by high local density and purity for further molecular and bacteria detection/analysis. *Published by AIP Publishing*. [http://dx.doi.org/10.1063/1.4953447]

INTRODUCTION

Rapid preconcentration of target cells/bacteria/biomolecules from a heterogeneous biosample plays an important role for further on-chip detection, analysis, and identification.[1–3] Immunoassays are typically used to specifically trap cells and biomolecules through an antibody-antigen reaction.[4] However, the long time required for consumption of the antibody-antigen reaction (>2 h) and low sensitivity limit its potential advantages for urgent diagnoses.[5] Surface-enhanced Raman spectroscopy (SERS) has been used for directly detecting and identifying bacteria/cells/molecules without complicated sample preparation and antibody-antigen reactions.[6–8] Unfortunately, Raman signals obtained from biological samples are very weak, especially in dilute samples. Furthermore, it is very difficult to directly identify pathogens/biomarkers from a heterogeneous sample using SERS, such as detection of bacteria/biomolecules in a blood sample.[9] Therefore, for practical on-chip molecular diagnosis (antibody-based and DNA-based) and SERS analysis, there is a critical need for separation and preconcentration of target cells from a heterogeneous sample in order to increase their local density on the sensing surface to raise both the reaction rate and sensitivity.

[a)]Author to whom correspondence should be addressed. Electronic mail: ifcheng@narlabs.org.tw

AC dielectrophoresis (DEP) is a non-damaging and non-contact method to induce particle movements toward relatively high or low electric field regions, and it is widely used for manipulating, separating, and concentrating bacteria, cells, molecules, and DNA[10–13] in such things as on-chip immunoassays, DNA hybridization, and opto–spectroscopy identification of bacteria/molecules/cells,[14–17] However, DEP works only in a short range because the decay relation of the electric field depends on the electrode shape and distance. The field strength decays with d^{-1} for a distant counter electrode.[11] For a 2D planar electrode configuration, the electric field also decays exponentially with the distance away from the electrodes along the z-direction.[11,14] Therefore, the short-range separation mechanism of the pure DEP technique makes it difficult to use in low concentration samples and wider reaction chambers. In addition, DEP force is as a function of particle volume ($F_{DEP} \sim r^3$). Therefore, DEP force is difficult to use for manipulating nanoscale particles, such as viruses, DNA, and proteins.[18,19] Considering the practical diagnostic applications, the detection target is typically at a very low concentration. Therefore, a long-range concentration is required to effectively transport a higher number of targets into a small detection area in order to increase sensor sensitivity.

AC electroosmosis (ACEO) is caused by the interaction between a non-uniform AC electric field and the electric double layer that is induced via accumulating charges near the surface of a polarized electrode. The ion migration drags the fluid to generate a surface-driven bulk flow over the electrode.[20] This effect is capable of generating long-range fluid convection, and thus, ACEO has been popularly used for microfluid transportation to collect protein/DNA/bacteria concentrations in a wider range with proper designs.[21–23] ACEO preconcentration provides high local density on the detection areas of a bench-based biochip intended to improve the detection limit for on-chip fluorescence-based, electrochemical impedance-based, SERS-based, and Quartz crystal microbalance (QCM)-based analysis of target particles.[24–28] However, a pure ACEO mechanism without selectivity makes it difficult to selectively manipulate and concentrate particles from a heterogeneous sample.

Our proposed approach combines the biased ACEO and DEP with a 3D convergency electric field design. In hybrid electrokinetics, ACEO provides long-range transportation, and DEP provides a separation mechanism, thus, resulting in a long-range and selective concentration of detection targets from a heterogeneous sample. Through a comb-shape convergency electrode design, target particles can transport along electrode surfaces to the center electrode over a long-range. The biased ACEO also provides a higher shear rate that prevents the target bacteria/nanocolloids from being attracted to the electrode edges by the positive DEP. In addition, a strong 3D negative DEP force on blood cells is higher than the biased ACEO drag, which can repel the blood cells away from the centre electrode. These two mechanisms result in high-purity selective concentration of target nanocolloids/bacteria into the centre electrode.

MATERIALS AND METHODS

Theory and chip design

A dielectric particle is induced the movements by non-uniform AC electric field-induced polarization, termed dielectrophoresis dielectrophoresis (DEP). The time averaged DEP force $F_{\mathrm{DEP}} = 2\pi r^3 \varepsilon_{\mathrm{m}} \mathrm{Re}[f_{CM}(\omega)] \nabla \mathrm{E}^2$ is dependent on the permittivity of the medium ε_{m}, the radius of the particle r^3, the effective polarizability (Clausius-Mossotti (CM) factor f_{CM}), and the magnitude of the electric field gradient $\nabla \mathrm{E}^2$. If particles are more polarizable than the surrounding medium, they will be attracted to a relatively strong electrical field gradient (positive DEP) region; if the particles are less polarizable than the surrounding medium, they will be pushed to a relative weak electrical field gradient (negative DEP) region. Therefore, the DEP mechanism can provide a precise separation in both the size and dielectric properties of a particle.[29] However, DEP works in a very short range due to the fact that the electric field decays exponentially with the distance from the 2D planar electrode along the z-direction,[11] thus causing particle separation to be characterized by a short range.

Ion migrations are generated as a result of the interaction between a non-uniform AC electric field and the induced electric double layer on the surface of a polarized electrode, which

drags fluid to generate a surface-driven bulk flow over the electrode, which is termed AC electroosmosis (ACEO). The flow velocity of ACEO can be described as follows:[20]

$$v_{ACEO} = \frac{\varepsilon V_o^2 \Omega^2}{8\eta x\left(1+\Omega^2\right)^2} \quad \Omega = \omega \frac{\varepsilon}{\sigma}\frac{\pi}{2} x\kappa. \tag{1}$$

The magnitude of ACEO velocity is dependent on the applied AC voltage V_0, the characteristic length of the electrode separation x, and the non-dimensional frequency Ω, which is dependent on the conductivity and permittivity of the medium and the Debye length k. The ACEO strength is frequency-dependent, and the frequency window of strong ACEO approximates to charge relaxation time that would shift to higher at a higher ion concentration of the medium.[20]

Asymmetric polarization generated by a DC bias applied with AC signals to induce capacitive charging and Faradaic charging on different electrodes.[21,30] This effect is capable of inducing fluid convection more effectively and can be used in a wider range of buffer conductivities to induce sufficiently high fluid convections.[30,31]

ACEO can induce a net flow to transport liquid samples in a wide range, but there is no specificity/selectivity for the particles in the fluid. By combining the short-range DEP that has discriminating capability with DC-biased Faradic Charging ACEO that has long-range transporting capability, target particles in a mixture sample can be selectively concentrated for subsequent analysis.

In this study, convergency electrode geometry was designed to generate a net flow toward the centre electrode due to the fact that the electric field strength is gradually increased from the outer to inner of the convergency electrode configuration. The tripolar electrode configuration (TEC) consists of a centre electrode, a convergency electrode around the centre electrode on the bottom layer, and a $\sim$1.5 cm^2 ITO glass on the top layer that fully covers the region of the bottom electrodes ($\sim$0.64 cm^2), as shown in Figs. 1(a) and 1(a-1). A patterned 200 μm 3M double-sided tape was used as a spacer between the top and bottom ITO electrodes to form a fluidic chamber (Fig. 1(a-1)).

The 3D electric field configuration generates an effective ACEO convection and 3D negative DEP force in the fluidic chamber. The 3D negative DEP force was induced between the circular electrode, the ring-shape (the end of the convergency electrode) electrode, and the top covered electrode to effectively repel blood cells away from the centre detection electrode in the 3D fluidic chamber, as shown in Figs. 1(a) and 1(c). The proposed design combines a short-range DEP and long-range AC electroosmosis (ACEO), which interact in coordination to rapidly and selectively concentrate the nano-molecules and bacteria from the diluted human blood sample. Due to the difference in the polarizability and size of the particles, the net force at a given locality can be in the direction toward the centre electrode for some particles and the direction away from the centre electrode for others (Figs. 1(a) and 1(b)). Therefore, the smaller target particles ranging from nanoscale to a few microns ($<$2 μm) can transport along the outer electrode into the centre electrode due to the induced high ACEO convection that gradually increases from outer to inner of the convergency electrode configuration (Fig. 1(b1)). The target particles could be conveyed along all of the tentacles of the radial electrode, and therefore, compared to the conventional circular electrode configuration, the working range of TEC ACEO was extended from a single circular electrode ($\sim$500 μm long) to a wide-rang radial electrode (diameter $\sim$8 mm long). This design and mechanism could convey a higher number of target particles to the detection surface of the middle circular electrode. A strong 3D repulsive DEP force on the blood cell ($>$5 μm) opposes and overwhelms the ACEO convective force toward the center electrode, and thus excluding the blood cells away from the center electrodes.

Sample preparation

Bacteria and 30 nm-fluorescent colloids were used to investigate the selective concentrations of the micro- and nano-scale particles from the diluted blood, respectively. *E. coli* (BCRC

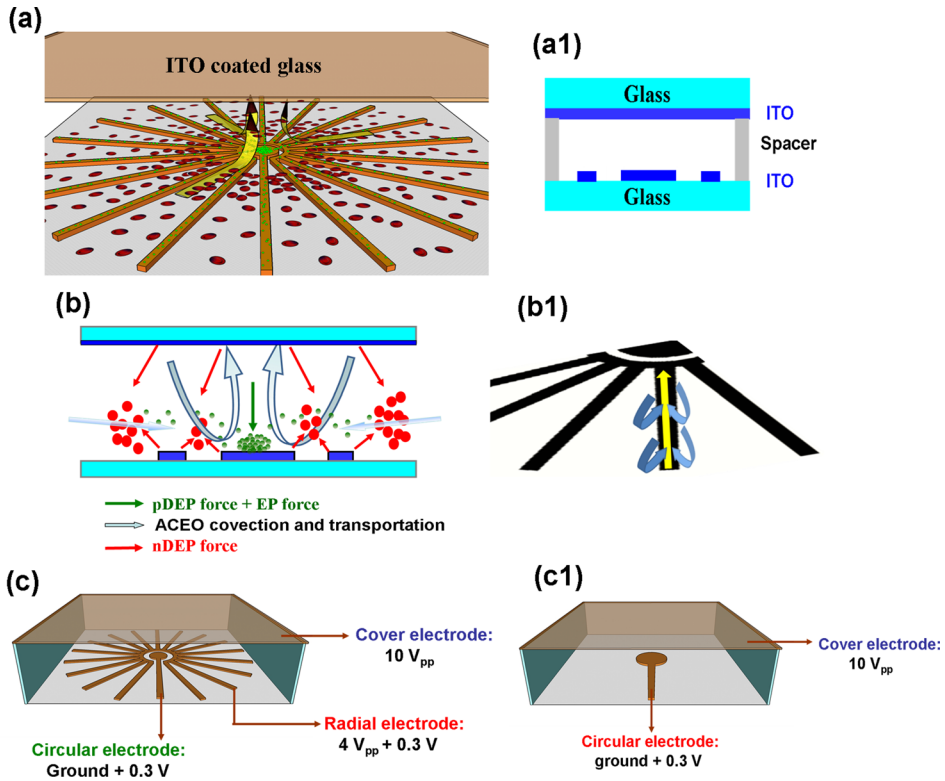

FIG. 1. (a) Illustration of the tripolar convergency electrode configuration to achieve long-range selective concentration of targets from blood cells. (a-1) Cross-sectional diagram of the biochip construction. (b) Illustration of the hybrid electrokinetic selective concentration mechanism under a long-range asymmetric electric field. (b-1) The long-range ACEO transports the smaller targets along the electrode from outer to inner of the convergency electrode configuration. (c) The setups of electric connections for long-range TEC and (c-1) short-range DEC, respectively.

15922, Gram negative) was cultured on tryptic soy agar (TSA) at 35 °C for over 18 h 30 nm fluorescent colloids were purchased from *Sigma* company (2.5%, solids-latex (w/w)). An isotonic solution phosphate buffered saline (PBS) solution diluted with 300 mM mannitol as an experimental buffer was adjusted to a conductivity of 250 μS/cm for the purpose of effectively driving the 3D hybrid electrokinetics. A mixed sample including nanocolloids at a concentration ranging from 2.5 ng/ml to 250 ng/ml, and blood cells at a concentration of 5×10^7 cells/ml was prepared to investigate optimal voltage, frequency, and the detection limit of the chip. The bacteria-blood cell mixture suspended in the experimental buffer was used for the purpose of investigating the behavior of the bacteria-blood cell separation mechanism. Bacteria and blood cell concentrations were adjusted to 2×10^5 CFU/ml and 2.5×10^8 cells/ml, respectively.

Chip fabrication and assembly

A face-to-face 3D electrode chip was manufactured via photolithography, ITO etching, and chip assembly. A positive photoresist (PR) AZ5214 was spin-coated on an ITO coated slide (76×26 mm and 700 μm thick), and then, the standard lithography, UV exposure (285 nm deep UV), and development processes were followed to determine the designed geometries on the ITO layer. After the photolithography, the exposed ITO layer was etched using 36% HCl, and the remaining PR was then removed by acetone to complete the microelectrode fabrication. The patterned ITO slide was bonded with another ITO slide via 200 μm thick double-sided tape (3M) to form a 3D non-uniform electric field gradient. The side view of the chip construction is shown in Fig. 1(a-1).

A multi-output function generator with four independent channels (FLUKE 284, FLUKE Calibration, USA) was used to support an output AC voltage range of 2–10 V and a DC bias of

0.3 V with a frequency range of 200 Hz–200 kHz. The applied voltages of 10 V_{pp}, 4 V_{pp}, and a ground with a DC bias of 0.3 V were applied to the top planar electrode, the bottom convergency electrode, and the central circular-shaped electrode, respectively, to generate a 3D electric field gradient. The setup of electric connection for long-range TEC is shown in Fig. 1(c), and a setup of electric connection for short-range dipolar electrode configuration (DEC) is shown in Fig. 1(c-1). The AC electrokinetic behavior of the bioparticles/nanocolloids was observed using an inverted microscope (IX 71, Olympus, Japan) with a fluorescent light source. The experimental results were recorded using a high speed charge-coupled device (CCD) camera (20 frames/s, DP-80, Olympus Japan), and the captured images were analyzed to obtain their relative fluorescence intensities via 8-bit gray-scale pixels using Image-Pro Plus 6.0 software (MediaCybernetics).

RESULTS AND DISCUSSION

Long-range hybrid electrokinetics for condensing target particles on a local area

In order to observe the transportation trajectory more clearly, 30 nm nanocolloids at a 50 ng/ml concentration spiked in a $\sim 5 \times 10^7$ blood cells/ml sample were used to investigate the long-range selective concentration of the nano-molecules in the 3D electrokinetic chip. A previous study mentioned that nano-scale colloids exhibit positive DEP at low frequency, and its cross-over frequency is with respect to the formation of the Debye length and the particle size. The nanocolloids showed evident positive DEP behavior in a frequency range between 100 Hz and 1 MHz.[32] The blood cells exhibited positive DEP behavior when the frequency was above 200 kHz and showed evident negative DEP force when the frequency was below 100 kHz. Besides, positive DEP behavior on bacteria was found at low and high frequencies in the prepared medium. Both bacteria and nanocolloids showed positive DEP characteristics below 10 kHz, and their magnitudes were much lower than the ACEO strength, as shown in Fig. 2(a). Therefore, the effective concentration of bacteria/nanocolloids to the middle stagnation point and exclusion of blood cells away from the detection surface could be achieved at the frequency range between 1 kHz and 10 kHz, as shown in Fig. 2(b). At the state of $F_{pDEP(target)} \approx F_{ACEO} < F_{nDEP(BC)}$ in Fig. 2(c), both types of particles experience stronger DEP forces repelling blood cells away from the middle of electrodes and attracting target particles as a ring-shape than the ACEO drag that moves them toward the central region. When the applied frequency is higher than 50 kHz, ACEO effect is disappeared, and the pure DEP effect cannot effectively concentrate the target particles to the centre region, as shown in Fig. 2(d).

The optimal condensation conditions should be frequency-dependent because both ACEO and DEP are very sensitive to the applied frequency of the AC voltage ($v_{DEP} \sim \nabla E^2$ and $v_{ACEO} \sim V_o^2$). To investigate an appropriate frequency by which the selective concentration can form a high density aggregate, various frequencies under constant applied voltages of 10 V_{pp}, 4 V_{pp}, and a ground with a DC bias of 0.3 V were applied to the top planar electrode, the bottom convergency electrode, and the central circular-shaped electrode, respectively, to generate a 3D electric field gradient. A frequency ranging from 0.2 kHz to 10 kHz was used to investigate the selective concentration and separation of the nanocolloids from a mixture sample of blood-nanocolloids. To reject the blood cells away from the detection area of the central electrode, the frequency range requires working in the range of a strong negative DEP force. To collect the detection targets, the applied electric conditions have to be adjusted in the range of an ACEO drag that is much higher than the positive DEP force on the nanocolloids.

The mixture of blood cells-nanocolloids was dropped into the 3D chip with a wide-range electrode configuration of Fig. 1(a). Figure 3(a) shows that the blood cells and nanocolloids were distributed randomly when no electric field was applied to the electrodes. The fluorescent nanocolloids were difficult to see due to the fact that the diffusion length of each molecule was longer than the length of the fluorescence scattering. Under an optimal frequency range between 1 kHz and 3 kHz, as shown in Fig. 3(b) for 2 kHz and after only 2 min, the nanocolloids were effectively transported along the convergency electrode and, finally, were concentrated onto a small area of the central electrode, while blood cells were excluded from all of the electrodes

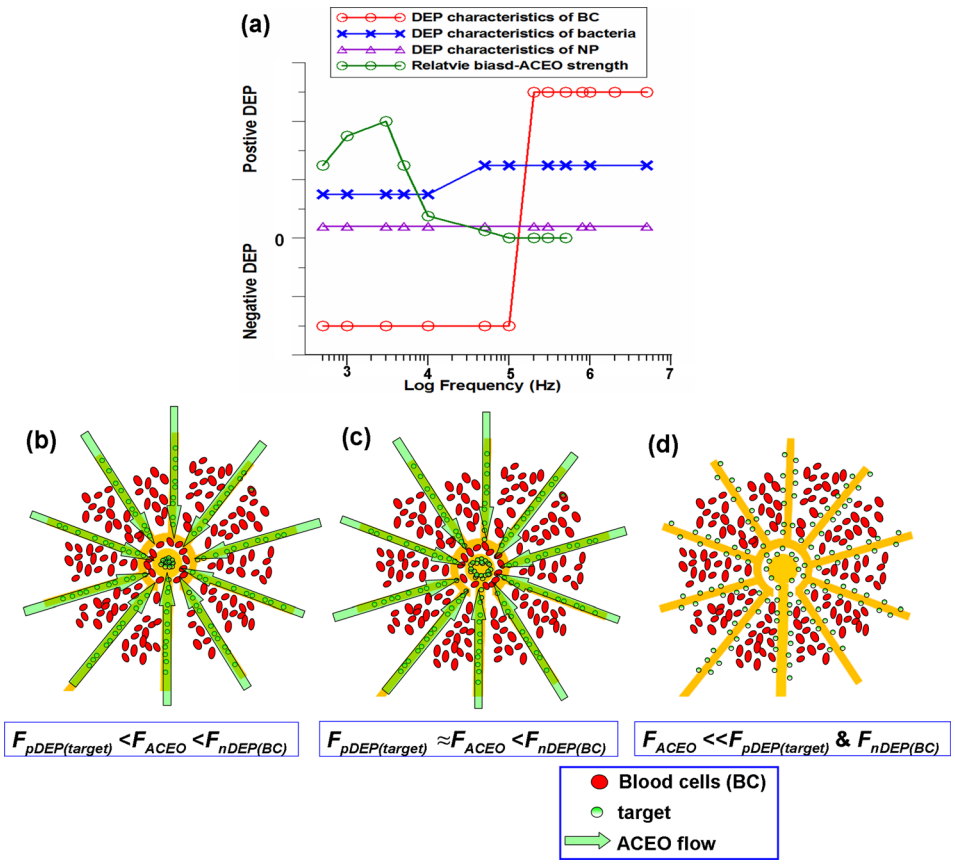

FIG. 2. (a) A sketched plot for positive/negative DEP and biased ACEO characteristics versus frequency on nanoparticles, bacteria and blood cells. (b) When $F_{pDEP(bacteria)} < F_{ACEO} < F_{nDEP(BC)}$, ACEO transport is higher than the positive DEP force on the target particles and lower than the opposite DEP force on the blood cell that allows the selective concentration of target particles at some specific electric field conditions. (c) At the state of $F_{pDEP(target)} \approx F_{ACEO} < F_{nDEP(BC)}$, both types of particles experience strong DEP forces repelling blood cells away from the middle of electrodes and attracting target particles as a ring-shape in the centre region. (d) When the applied frequency is higher than 50 kHz, ACEO effect is disappeared, and the pure DEP effect cannot effectively concentrate the target particles.

and were especially strongly pushed away from the centre electrode. Even though some blood cells could also be slightly convected toward the centre direction by the lateral ACEO drag force, however, a significant negative DEP force prevented them from entering into the centre electrode (Multimedia view). This image is enhanced as a video in the supplemental material. When the predetermined electric condition was applied at a frequency of 0.2 to 1 kHz, the blood cells induced negative DEP, and the nanomolecules induced a positive DEP force; both types of particles experience stronger DEP forces than the ACEO drag, resulting in the blood cells being repelled away from the electrodes and attracting the nanocolloids to form as a ring-shape aggregate, as shown in Fig. 3(c). This is because the extremely high positive DEP force and the electrophoretic force induced near the electrode edges at low frequencies caused a concentration effect that could not focus on a small spot, thus forming a circular ring inside the centre electrode. When the applied frequency was above 3 kHz, the magnitude of ACEO decreased, and this effect also caused positive DEP force on the target colloids was higher than the ACEO drag, thus, producing the same trapping phenomenon with the result of the applied frequency between 0.2 and 1 kHz.

Comparison of the concentration efficiency of the short-range and long-range designs

30 nm fluorescence colloidal particles were spiked in diluted blood for the purpose of investigating the concentration efficiencies of short-range and long-range electric field designs.

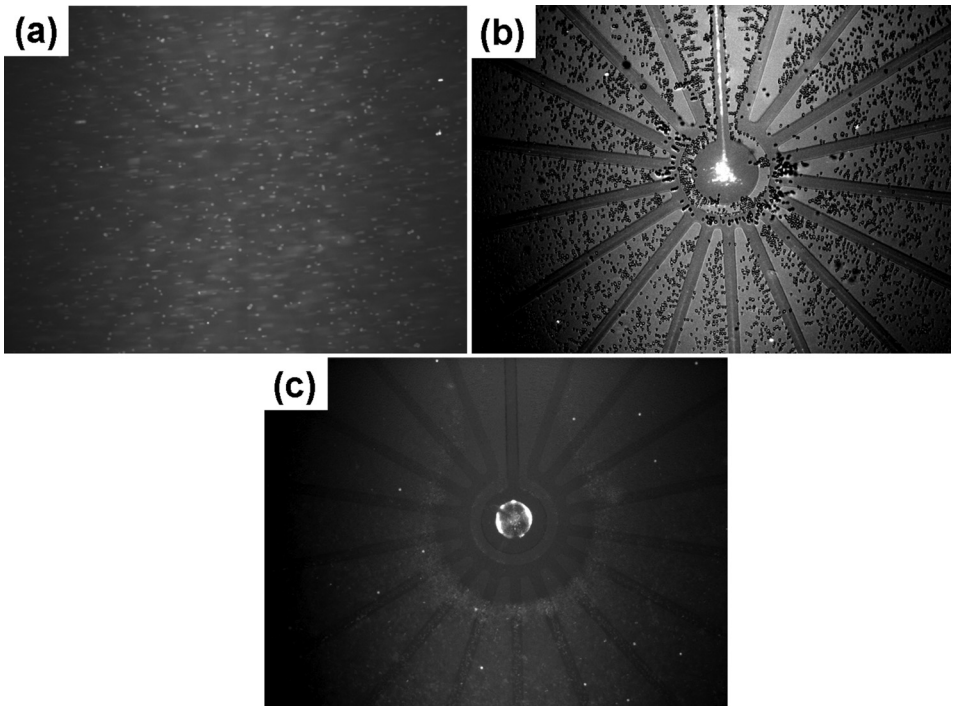

FIG. 3. (a) Both blood cells and fluorescent nanocolloids were distributed randomly when no electric field was applied. (b) In a frequency range between 1 and 3 kHz, fluorescent nanocolloids were conveyed along the electrodes and concentrated onto the centre electrode, and blood cells were excluded away from the electrodes (Multimedia view). This image is enhanced as a video in the supplemental material. (c) When the applied frequency was below 1 kHz and above 3 kHz, the higher positive DEP and electrophoretic forces as compared to the ACEO drag caused the formation of concentrated nanocolloids in the form of a ring-shape. (Multimedia view) [URL: http://dx.doi.org/10.1063/1.4953447.1]

Firstly, 100 ng/ml fluorescent nanocolloids were concentrated by using a dipolar electrode configuration (DEC) generated 3D electric field that was constructed with a 500 μm diameter circular electrode at the bottom and a 1 cm^2 area ITO glass on the top of a reaction chamber. The results show that fluorescent nanocolloids were rapidly concentrated to the central region of the circular electrode, and the fluorescent intensity reached a plateau after applying the electric field for only ~1 min (Figs. 4(a) and 4(a-1)). Furthermore, nanocolloids with the same concentration were continuously concentrated using a 3D tripolar electrode configuration (TEC) generating a long-range electric field, and the fluorescence intensity increased more quickly and reached a plateau after applying voltage for ~ 4 min, as shown in Fig. 4(a). Compared to the DEC 3D electric field, the TEC induced a longer range 3D electric field to transport a greater number of target colloids to the centre electrode. In addition, due to the fact that longer distance transportation should require more transportation time, the 8 mm long concentration reached a plateau that required a longer time than the 0.5 mm short range concentration, but it appeared as a much higher fluorescence intensity, as shown in Fig. 4(a-2).

The nanocolloid concentration was adjusted from 1 to 250 ng/ml to investigate the detection limits of the 3D short-range and long-range chips. Figure 4(b) shows the experimental results for fluorescent intensity versus different nanocolloid concentrations after electrokinetic concentration for 5 min using the 3D DEC chip and 3D TEC chip, respectively. The results show that the fluorescence intensities collected using TEC long-range condensing were 5–8 times higher than those collected using DEC short-range condensing at high concentrations of 100–250 ng/ml and were 6–10 times higher at concentrations of 10–50 ng/ml. The detection limit of the DEC short-range concentration was 25 ng/ml, and the detection limit of the TEC long-range concentration reached 2.5 ng/ml (Fig. 4(b1)). The concentration capability of the TEC configuration increased roughly 10 times. This was attributed to the 8 mm long-range chip that could electrokinetically transport a higher number of targets than the 0.5 mm short-range chip.

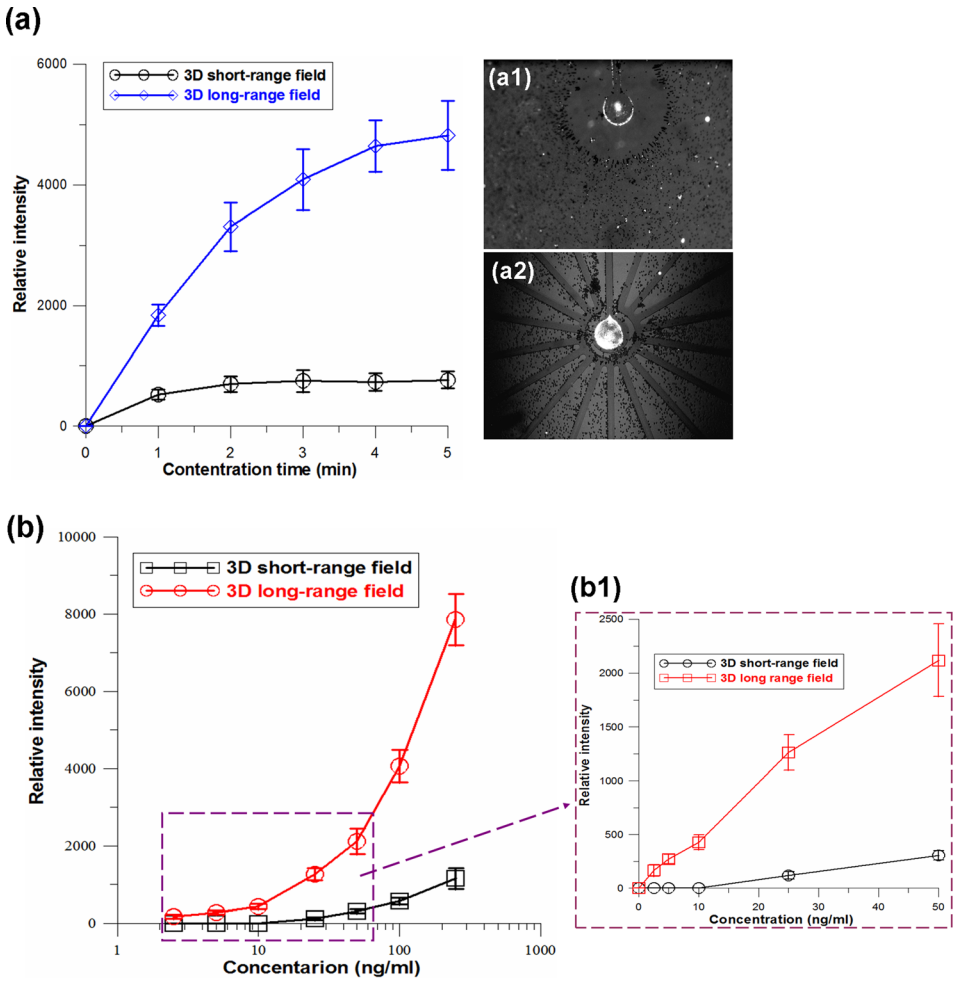

FIG. 4. (a) Intensity accumulation profiles obtained by continuous pre-concentration of nanocolloids from diluted blood using 3D DEC (a-1) and TEC (a-2) chips, respectively. (b) Fluorescence intensity versus different nanocolloid concentrations. The florescence intensity was measured after electrokinetic concentration of nanocolloids from the diluted blood for 5 min using the 3D short-range DEC and long-range TEC chips, respectively. (b-1) The linear scale data in a range between 2.5 and 50 ng/ml. The detection limit of the 3D short-range DEC and long-range TEC electrokinetic concentrations reached 25 ng/ml and 2.5 ng/ml, respectively.

Capability of bacteria concentration and blood cell rejection using 3D hybrid electrokinetics

S. aureus (bacteria concentration $\sim 2 \times 10^5$ CFU/ml) spiked in diluted blood was used to demonstrate the selective concentration capability for pathogen detection. The final concentration of *S. aureus* and blood cells was adjusted to 10^5 and 2×10^8 cells/ml, respectively. In our experimental buffer, the blood cells exhibited a strong negative DEP force at a frequency range between 300 Hz and 100 kHz, and the bacteria induced a positive DEP force at both high and low frequencies. Hybrid-electrokinetics depends on the frequency of the applied voltage as well as the size/dielectric properties of the particle under consideration. Therefore, the frequency-dependent DEP and ACEO regulated the relative magnitudes and opposite directions of the induced forces in bacteria and blood cells for the purpose of size separation and selective concentration. If the applied frequency was lower than 1 kHz, the bacteria and blood cells experienced stronger positive and negative DEP forces, respectively, that were higher than the ACEO drag ($F_{pDEP(bacteria)}$ and $F_{nDEP(BC)} > F_{ACEO}$), which resulted in trapping bacteria as a ring-shape and repelling the blood cells near the centre electrode, similar to the state in Fig. 3(c) (data not shown). This mechanism cannot condense the bacteria on a small area. Under an optimal

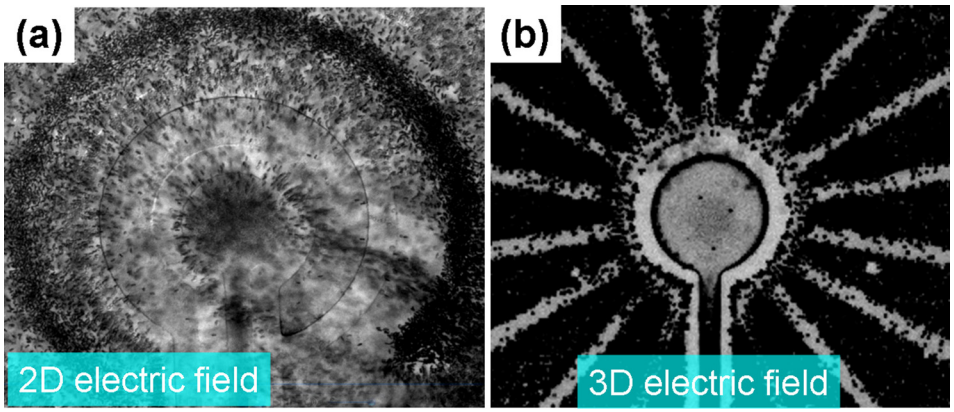

FIG. 5. (a) 2D planar concentric electrode configuration shows poor blood cell rejection due to the fact that the DEP force decays exponentially with the distance from the electrodes along the z-direction. (b) 3D long-range TEC chip demonstrated excellent concentration capability and blood cell rejection rate for further analysis of the detection target.

frequency range between 1 kHz and 3 kHz, a 2D planar concentric electrode configuration as discussed in our previous report[25] was used to compare the depletion capability of blood cells with the proposed 3D TE configuration. The experimental results showed poor blood cell rejection using a 2D planar concentric electrode due to the fact that the DEP force generated by the planar electrodes decayed exponentially with the distance from the electrodes along the z-direction. The field decay in z-direction resulted in a significant reduction in the purity of the condensed slug in the centre electrode (Fig. 5(a)). Nevertheless, using the 3D convergency electrode configuration to concentrate the bacteria at a frequency of 2 kHz, the hybrid electrokinetics transported the bacteria along the convergency electrode toward the centre area because the strong ACEO drag was much higher than the positive DEP force on the bacteria pulling the bacteria onto a stagnation area at the center of the electrode. In the meantime, the blood cells were repelled away from the centre electrode because the induced 3D negative DEP force on the blood cells was much higher than the ACEO dynamics (Fig. 5(b)). Compared to the original random distribution, there was a high density of bacteria at the center of the centre electrode, and the concentration factor carried out by the proposed 3D hybrid electrokinetics increased several orders of local density and raised the local purity at least 6 orders (from 0.05% to greater than 99.9%). The blood cell rejection rate of the 3D hybrid electrokinetic concentration was much higher than that of the 2D planar hybrid electrokinetic concentration, as shown in Figs. 5(a) and 5(b). The excellent concentration capability characterized by long-range, high selectivity shows good feasibility and advancement for further on-chip SERS or FTIR identification of pathogens in blood.[27,33] In approximately 90% of bacteremia patients, only single pathogenic species can be found at a time;[35] it is rare to see the mixed infection in a blood sample.[36] Thus, effectively concentrating bacteria in a blood sample is a useful platform for further identification. For molecular detections, the target molecules can be specific trapped via the use of antibodies and probes. Our proposed selective concentration can greatly reduce the interference from the dense blood cells or impurities, and the condensing effect on the detection surface can also accelerate the reaction rate of affinity and improve the detection limit.

CONCLUSIONS

The proposed 3D hybrid electrokinetic concentration was demonstrated for the purpose of selectively condensing particles at a scale between nanometers (molecules) and micrometers (bacteria) from diluted blood. Through a homocentric convergency-shaped electrode design, the chip achieved the long-range transportation of target bioparticles to a small sensing area, wherein the blood cells were repelled away from the sensor surface for further highly sensitive detection. The appropriate situation occurred at a significant ACEO convection that was higher than the positive DEP force on the nanocolloids/bacteria and a lower ACEO drag force than the

opposite DEP force on the blood cells. The couple effect allowed the selective concentration of nanocolloids/bacteria at specific frequencies of the applied voltage. The concentration capability of 3D TEC long-range electrokinetic concentration was one order higher than that of the 3D DEC short-range electric field concentration. Compared to a conventional 2D concentric electrode, the 3D electric field distribution significantly raised the rejection efficiency of blood cells through the use of the hybrid electrokinetics. These two complex advancements in a 3D hybrid electrokinetic biochip, long-range and high-purity selective concentration of the particles in a range from nanoscale to microscale, could be carried out for high performance detection of bacteria/biomarkers/DNAs/virus in diluted blood or serum. A minute-level speed immunoassay and the on-chip identification of biological cells are undergoing. This platform has high potential to be conducted with optical, physical, or electrical detection methods to develop rapid and highly sensitive diagnostic assays.[26,27,34]

ACKNOWLEDGMENTS

This work was supported by the Ministry of Science and Technology of Taiwan (MOST 104-2221-E-492-009-MY2 and MOST 102-2221-E-492-001-MY2). We also thank the National Nano Device Laboratory for supplying the micro-fabrication equipment.

[1]R. Vaidyanathan, S. Dey, L. G. Carrascosa, M. J. A. Shiddiky, and M. Trau, Biomicrofluidics **9**, 061501 (2015).
[2]Z. Slouka, S. Senapati, S. Shah, R. Lawler, Z. Shi, M. S. Stack, and H.-C. Chang, Talanta **145**, 35–42(2015).
[3]Y. Hua, A. B. Jemere, J. Dragoljic, and D. J. Harrison, Lab Chip **13**, 2651 (2013).
[4]D. S. Hage, Anal. Chem. **67**, 455–462 (1995).
[5]K. Kerman, M. Vestergaard, and E. Tamiya, Methods Mol. Biol. **504**, 99–113 (2009).
[6]S. Tian, Q. Zhou, Z. Gu, X. Gu, and J. Zheng, Analyst **138**, 2604–2612 (2013).
[7]Z. A. Nima, M. Mahmood, Y. Xu, T. Mustafa, F. Watanabe, D. A. Nedosekin, M. A. Juratli, T. Fahmi, E. I. Galanzha, J. P. Nolan, A. G. Basnakian, V. P. Zharov, and A. S. Biris, Sci. Rep. **4**, 4752 (2014).
[8]S. M. Yoo and S. Y. Lee, Trends Biotechnol. **34**, 7–25 (2016).
[9]T.-Y. Liu, K.-T. Tsai, H.-H. Wang, Y. Chen, Y.-H. Chen, Y.-C. Chao, H.-H. Chang, C.-H. Lin, J.-K. Wang, and Y.-L. Wang, Nat. Commun. **2**, 538 (2011).
[10]Z. R. Gagnon, Electrophoresis **32**, 2466 (2011).
[11]I-F. Cheng, W.-L. Huang, T.-Y. Chen, Y.-D. Lin, C.-W. Liu, and W.-C. Su, Lab Chip **15**, 2950 (2015).
[12]Y.-H. Su, M. Tsegaye, W. Varhue, K.-T. Liao, L. S. Abebe, J. A. Smith, R. L. Guerrant, and N. S. Swami, Analyst **139**, 66 (2014).
[13]A. Rohani, W. Varhue, Y.-H. Su, and N. S. Swam, Biomicrofluidics **8**, 052009 (2014).
[14]A. Sonnenberg, J. Y. Marciniak, R. Krishnan, and M. J. Heller, Electrophoresis **33**, 2482 (2012).
[15]K.-T. Liao and C.-F. Chou, J. Am. Chem. Soc. **134**, 8742 (2012).
[16]C.-H. Chuang, H.-P. Wu, Y.-W. Huang, and C.-H. Chen, Biosens. Bioelectron. **48**, 158 (2013).
[17]Y.-L. Deng and Y.-J. Juang, Biomicrofluidics **7**, 014111 (2013).
[18]I-F. Cheng, T.-Y. Chen, R.-J. Lu, and H.-W. Wu, Nanoscale Res. Lett. **9**, 324 (2014).
[19]L. F. Zheng, S. D. Li, P. J. Burke, and J. P. Brody, in *Proceedings of the 3rd IEEE Conference on Nanotechnology, San Francisco, 12–14 August 2003*, Vol. 2, pp. 437–440.
[20]N. G. Green, A. Ramos, A. Gonza'lez, H. Morgan, and A. Castellanos, Phys. Rev. E **61**, 4011–4018 (2000).
[21]J. Wu, IEEE Trans. Nanotechnol. **5**, 84–89 (2006).
[22]M. L. Y. Sin, V. Gau, J. C. Liao, D. A. Haake, and P. K. Wong, J. Phys. Chem. C **113**, 6561–6565 (2009).
[23]M. R. Bown and C. D. Meinhart, Microfluid. Nanofluid. **2**, 513–523 (2006).
[24]R. Hart, R. H. Lec, and M. Noh, Sens. Actuators, B **147**, 366–375 (2010).
[25]I-F. Cheng, S.-L. Yang, C.-C. Chung, and H.-C. Chang, Analyst **138**, 4656 (2013).
[26]R. Hart, E. Ergezen, R., Lec, and H. M. Noh, Biosens. Bioelectron. **26**, 3391 (2011).
[27]I-F. Cheng, H.-C. Chang, T.-Y. Chen, C. Hu, and F.-L. Yang, Sci. Rep. **3**, 2365 (2013).
[28]C.-C. Wu, W.-C. Huang, and C.-C. Hu, Sens. Actuators, B **209**, 61 (2015).
[29]S.-H. Liao, I.-F. Cheng, and H.-C. Chang, Microfluid Nanofluid **12**, 201 (2012).
[30]M. Lian and J. Wu, Appl. Phys. Lett. **94**, 064101 (2009).
[31]J.-K. Chen, C.-N. Weng, and R.-J. Yang, Lab Chip **9**, 1267 (2009).
[32]S. Basuray, H.-H. Wei, and H.-C. Chang, Biomicrofluidics **4**, 022801 (2010).
[33]P. Zarnowiec, L. Lechowicz, G. Czerwonka, and W. Kaca, Curr. Med. Chem. **22**, 1710 (2015).
[34]S. Krishnamoorthy, A. A. Iliadis, T. Bei, and G. P. Chrousos, Biosens Bioelectron. **24**, 313 (2008).
[35]N. Wellinghausen, A.-J. Kochem, C. Disqué, H. Mühl, S. Gebert, J. Winter, J. Matten, and S. G. Sakka, J. Clin. Microbiol. **47**, 2759 (2009).
[36]A. Pechorsky, Y. Nitzan, and T. Lazarovitch, J. Microbiol. Methods **78**, 325 (2009).